

Supporting Information
to the paper entitled

Effective perspiration is essential to uphold the stability of
zero-gap MEA-based cathodes used in CO₂ electrolyzers

H. Hu, Y. Kong, M. Liu, V. Kolivoška, A. V. Rudnev, Y. Hou, R. Erni, S. Vesztergom, P.
Broekmann

Contents

| | |
|---|---|
| Fig. S1. Model electrolysis studies at different current densities | 2 |
| Fig. S2. TEM characterization of PVP-capped Ag NPs (10 nm size) | 2 |
| Fig. S3. TEM characterization of BPEI-capped Ag NPs (50 nm size) | 3 |
| Fig. S4. EDX investigation of penetration depths, 10 nm and 100 nm PVP-capped Ag NPs | 3 |
| Fig. S5. Electrolysis stress-tests, 100 nm PVP-capped Ag NPs | 4 |

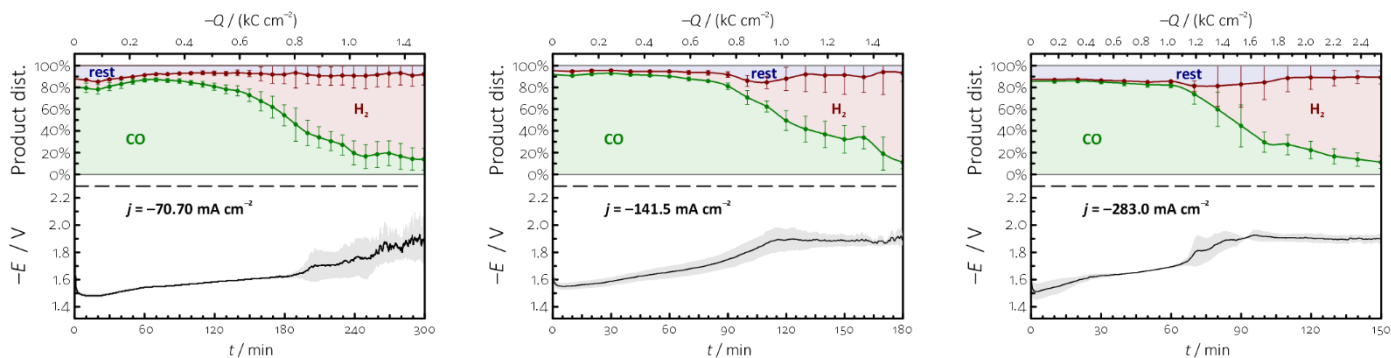


Fig. S1. The results of electrolysis stress-tests using PVP-deficient Ag NPs of 10 nm nominal size as catalyst. Upper panels show the product distribution of the electrode reaction, lower panels the change of the electrode potential E . The application of higher current densities leads earlier to erratic cell behavior; the surface area-normalized charge scale provides, however, better comparability. These experiments were carried out in the zero-gap cathode MEA-based model electrolyser shown in Fig. 1 of the main document, with a small effective cross-section. Due to more pronounced edge effects, stability issues manifest early (in hours rather than in days), enabling accelerated durability studies.

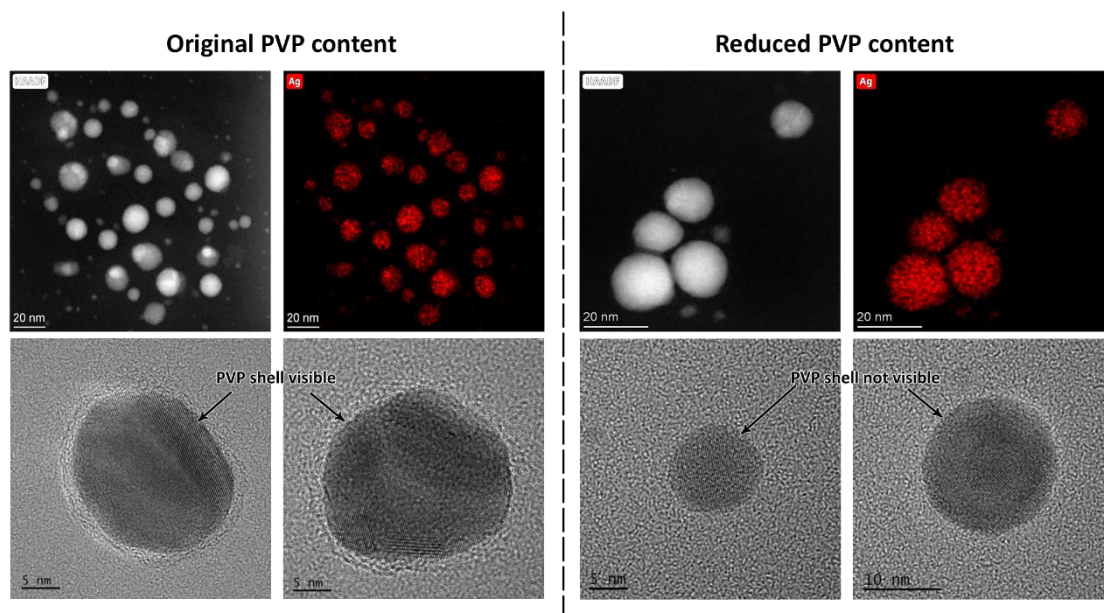


Fig. S2. Scanning Transmission Electron Microscopy (STEM)/EDX and high resolution Transmission Electron Microscopy (TEM) images of PVP-capped Ag NPs of 10 nm nominal diameter. Colored images show elemental maps of Ag (in red). To the left: NPs of the original (as-purchased) suspension; to the right: NPs of re-dispersed suspensions that underwent ultracentrifugation-based PVP removal.

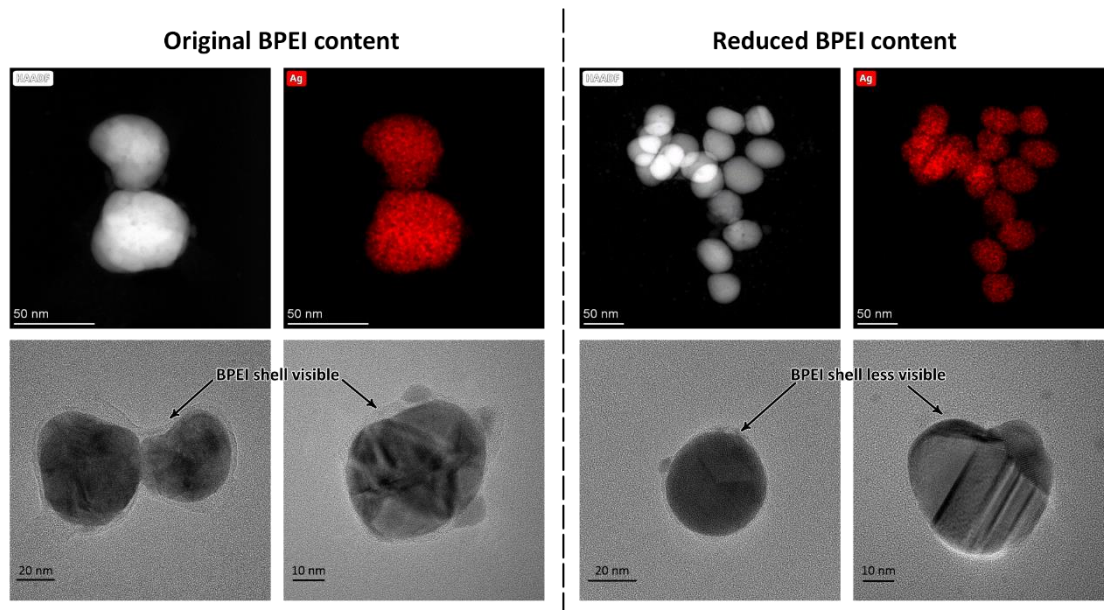


Fig. S3. Scanning Transmission Electron Microscopy (STEM)/EDX and high resolution Transmission Electron Micrograph (TEM) images of BPEI-capped Ag NPs of 50 nm nominal diameter. Colored images show elemental maps of Ag (in red). To the left: NPs of the original (as-purchased) suspension; to the right: NPs of re-dispersed suspensions that underwent ultracentrifugation-based BPEI removal.

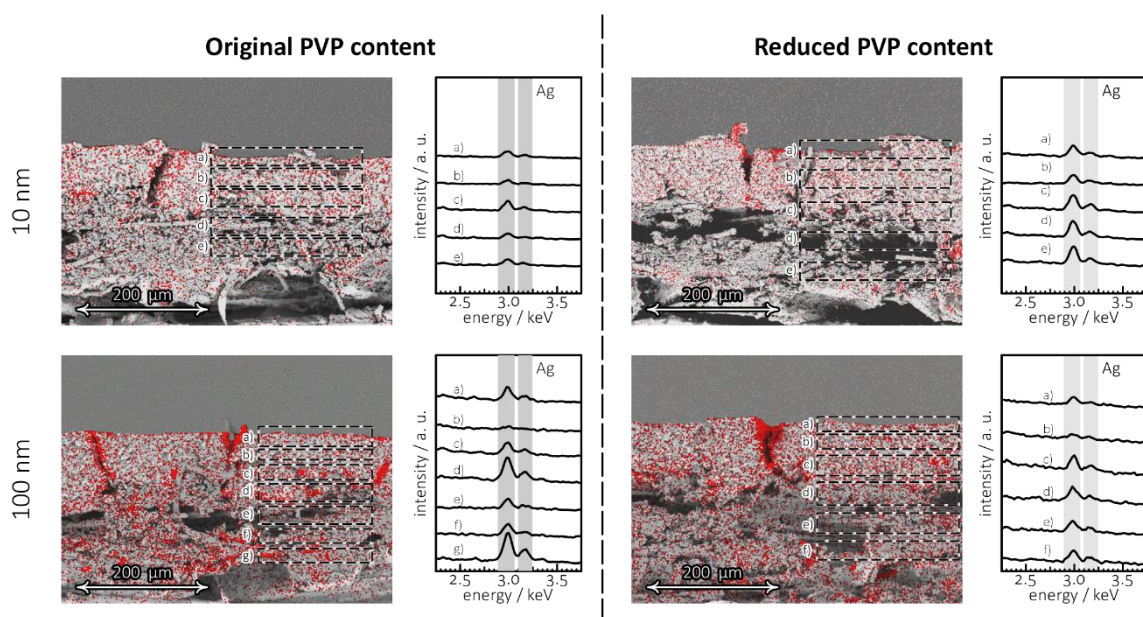


Fig. S4. Cross-sectional EDX maps of GDEs prepared with Ag NPs of different nominal sizes, without (to the left) and with (to the right) ultracentrifugation-based removal of the excess PVP content. The EDX spectra show that Ag NPs of 10 nm diameter penetrate more the microporous layer than the larger NPs of 100 nm size. The latter rather stay concentrated in the catalyst layer (on-top of the MPL) or reach deeper layers (as deep to the carbon fibrous layer) by penetrating larger voids (cracks).

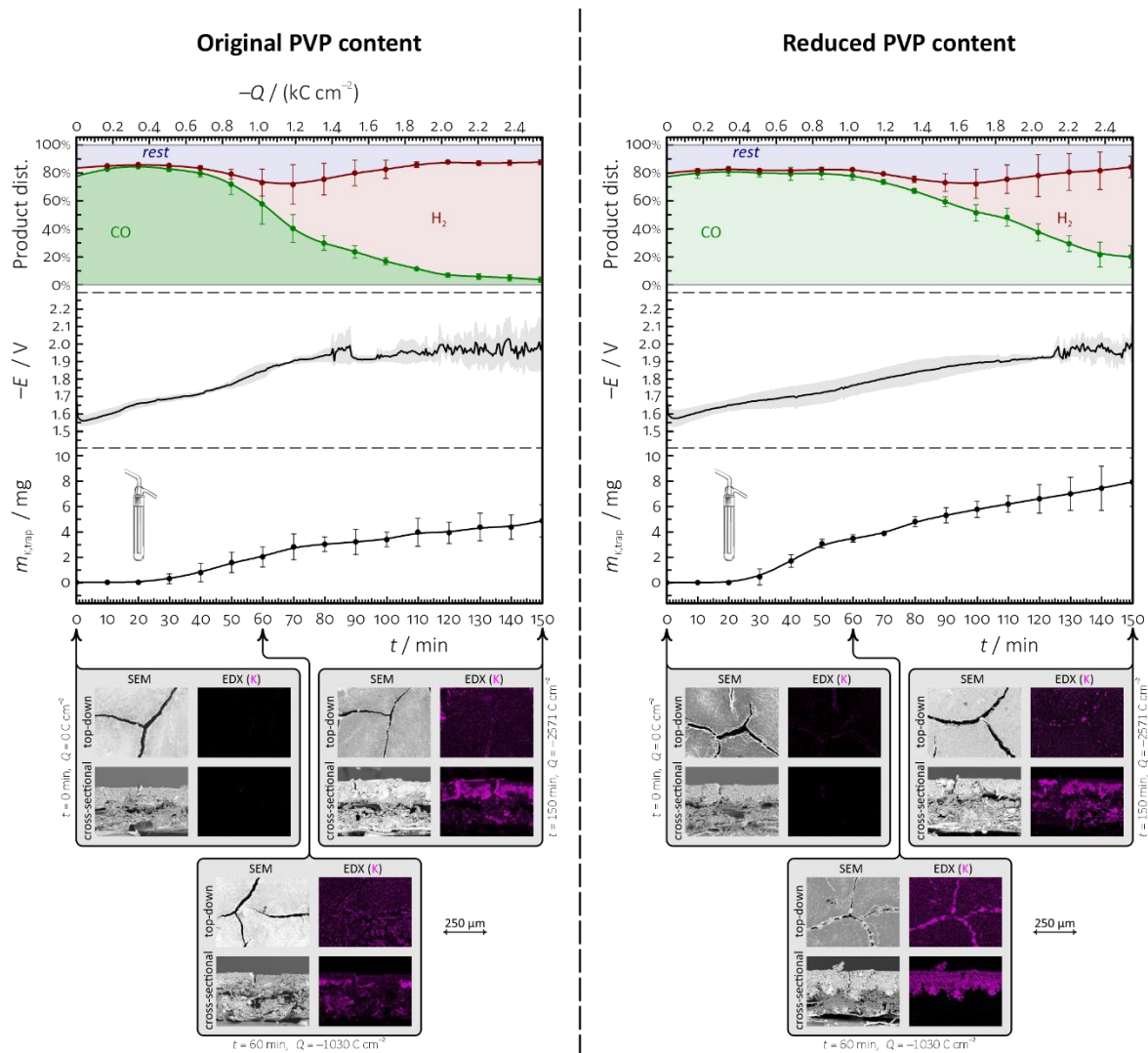


Fig. S5. Comparison of the results of electrolysis stress-tests on two different GDEs prepared with PVP-capped Ag NPs of 100 nm nominal diameter. The PVP content of the Ag NP suspensions was either unchanged (left side) or was reduced by ultracentrifugation (right side) during the course of catalyst ink preparation; in both cases, the catalyst was applied at a mass loading of $300 \mu\text{g cm}^{-2}$ Ag. The plots show the variation of the product distribution of CO₂ reduction, the measured electrode potential E (referenced vs. an Ag | AgCl | 3 mol dm⁻³ KCl electrode), and the mass of K⁺ ions collected in the liquid trap equipped to the gas outflow of the electrolyser, as a function of both time and passed charge, for galvanostatic electrolyses carried out at -283 mA cm^{-2} . Structural changes of the applied GDEs were monitored by recording top-down and cross-sectional SEM/EDX images of the GDEs obtained before, as well as 60 and 150 mins after the electrolysis.